Surface tracking in coherence scanning interferometry by B-Spline model and Teager-Kaiser operator

Fabien Salzenstein[1], Hassan Mortada[2], Vincent Mazet[3], Manuel Flury[4]
[1]*Université de Strasbourg, laboratoire ICube, 23 rue du Loess, Strasbourg, 67037 Cedex 2, France*
[2]*Exail Technologie, 34 rue de la Croix de fer, Saint Germain en Laye, 78100, France*
[3] *Telecom Physique Strasbourg, laboratoire ICube, 300 Bd Sbastien Brant, 67400, Illkirch-Graffenstaden, France*
[4]*Institut National des Sciences Appliquées, laboratoire ICube, 24 Bd de la Victoire, Strasbourg, 67000, France*
f.salzenstein@unistra.fr,Hassan.Mortada92@gmail.com, vincent.mazet@unistra.fr, manuel.flury@insa-strasbourg.fr

Keywords: AM-FM model, B-Spline, Teager-Kaiser energy operator, Surface extraction

Abstract: This work deals with the challenge of surface extraction using a combination of Teager-Kaiser operators and B-splines in the context of coherence scanning (or white light scanning i.e, WLSI) interferometry. Our approach defines a B-spline regularization model along surface profiles extracting their features by means of parameters locally describing fringe signals along the optical axis, while most studies are limited to a one-dimensional signal extraction. In doing so, we take into account four characteristic parameters under Gaussian hypothesis. The interest of the proposed strategy consists in processing the layers present in a material, in a context of soft roughness surfaces. The efficiency of our unsupervised method is illustrated on synthetic as well on real data.

1 Introduction

1.1 Context

White light scanning interferometry (WLSI) is a technique for analyzing material surfaces, particularly to estimate their roughness or shape. It can supplement the manufacturing control of new materials, microelectronic devices and microelectromechanical systems (MEMS) (O'Mahony et al., 2003). In addition, methods based on the AM-FM model of the interference signal along the optical axis allow an accurate precision. Thus, the information about the depth of the material can be extracted simultaneously from the envelope and the phase of the AM-FM signal. Plenty of algorithms, whether based on envelope detection (Larkin, 1996; Sandoz, 1997), frequency domain analysis (de Groot and Deck, 1993; de Groot et al., 2002), correlation with a reference fringe (Chim and Kino, 1990), Hilbert transformation (Pavliček and Michalek, 2012), TK algorithm (Gianto et al., 2016), extraction of the phase information (Guo et al., 2011), Kalman approach (Gurov et al., 2004), have been proposed, proceeding along the optical axis i.e, thus corresponding to 1D approach. Additionally 2D techniques have been presented (Gurov and Volynsky, 2012; Zhu and Wang, 2012). Due to its simplicity of implementation, adapted to the AM-FM signal model, the nonlinear Teager-Kaiser energy operator (TK or TKEO) (Vakman D., 1996; Maragos P. et al., 1993) seems to be effective (Larkin, 1996; Salzenstein et al., 2014) as well in its bi-dimensional (Boudraa et al., 2005) or multidimensional version (Salzenstein and Boudraa, 2009). In particular, most of these methods undertake to measure the roughness of surfaces, namely the evolution of their depth according to the lateral directions. We believe that approaches, which may take into account both lateral and height information, namely 2D or even 3D processing over the entire data cube, are potentially more suitable than one-dimensional approaches, in order to track surfaces, especially when they own low roughness. Our study focuses on a new 2D method, adapted for such surfaces.

1.2 Objectives

In order to ensure a good surface tracking, taking into account the neighborhood information along the lateral axis, by a regularization approach, we propose to describe four characteristic parameters of AM-FM signals under the hypothesis of a Gaussian envelope, by introducing a B-spline modeling, combined with the TK operator. A study based on spectral tracking has been carried out in the field of astronomy, pro-

viding solutions to close problems (considering spectral data) although signals do not contain any carrier term (Mortada et al., 2018). B-splines have proven their effectiveness in many areas of signal processing. One of their common applications consists in interpolation (Reinsch, 1967; Unser, 1999), which is helpful to find pixel values at continuous positions after some geometric transformations, for image resizing and resampling. They have also found other application in image registration (Rueckert et al., 2006), edge detection (Mallat and Zhong, 1992), signal compression (Medioni and Yasumoto, 1987), 3D modeling (Hoch et al., 1994). In the field of coherence scanning interferometry, this approach has been helpful to improve the interference signal (Duan et al., 2023) on the optical axis (depth) in the context of least squares phase shift methods (as well for continuous phase estimation related to the noisy fringe patterns in digital speckle interferometry (Wielgus et al., 2014)) or to approximate local detected envelope (Montgomery et al., 2013). B-spline technique has been proposed to fit surfaces, without taking into account the physical local model of the interference signal (Bruno, 2007). To the best of our knowledge, no global approach has been proposed modeling four characteristic parameters (surface position, amplitude, variance, carrier frequency) by B-splines, under the assumption of locally Gaussian envelopes: this deals with the main contributions of our study, in combination with a TK technique. The remainder of the paper is organized as follows: after the presentation of the context of the interferometric data in section 2 we recall TK algorithm and B-spline approach, respectively in section 3 and 4. An unsupervised model adapted to our data has been detailed in section 5. Finally, results on both synthetic and real images are presented in section 6.

2 Interferometric signal

Figure 1 shows the typical layout of WLSI device using the z-scan technique. By means of a single vertical scan of the sample, over the whole depth of the surface by modifying the distance between the objective and the sample, a stack of xyz images is produced. The resulting signal corresponds to the sum of the interferences at each wavelength. From such a signal, the objective is to extract depth information related to the analyzed surfaces. For surface roughness measurement, a classic signal processing technique generally aims to provide position at the maximum of the single fringe envelope along the depth handled by the optical axis z for each lateral coordinate (x,y), which represents the horizontal extent of a material sample. Therefore, the (relatively) greater the variation in surface height between neighboring lateral sites, the rougher it will be considered.

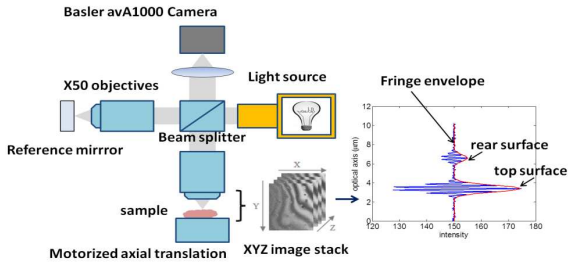

Figure 1: Schematic layout of WLSI system. The right hand pattern represents an interference signal along the depth axis z for two layers of surfaces, at a given (x,y) position.

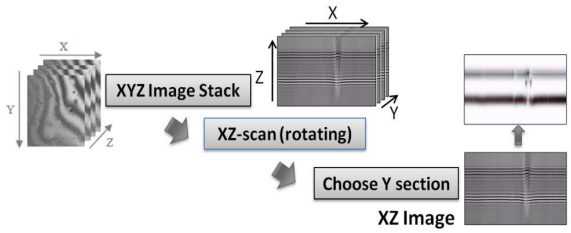

Figure 2: Recovery and process of a 2D xz image from a 3D xyz block generated by the WLSI interferometric system.

A typical intensity signal obtained from a digital camera when the OPD (optical path difference) varies in the interferometer at a given point (x,y) on the material surface, can be approximated along the optical z axis by a such modulated sinusoid (Larkin, 1996):

$$s(x,y,z) = a(x,y,z) + \underbrace{b(x,y)\exp\left[-\left(\frac{z-h(x,y)}{l_c}\right)^2\right]}_{C(x,y,z)} \times \cos\left[\frac{4\pi}{\lambda_0}(z-h(x,y)) + \alpha(x,y)\right]$$

where z is a vertical scanning position along the optical axis, $h(x,y)$ represents the height of the surface, $a(x,y,z)$ is an offset intensity containing low frequency components, $b(x,y)$ is a factor proportional to the reflected beam intensity, and $\alpha(x,y)$ is an additional phase offset and $C(x,y,z)$ is the envelope. The parameter l_c represents the coherence length and λ_0, the average wavelength of the light source. Generally the phase offset varies slowly from one point (x,y) to the next, and can be neglected, since only relative heights of the surface matter. The main challenge consists in determining the height at each point of the surface by exploiting the information provided by both the envelope or the phase simultaneously.

3 Teager-Kaiser energy operators

TKEOs algorithms (Boudraa and Salzenstein, 2018) are non-linear methods for envelope detection and phase retrieval from AM-FM signals such as those given by Eq. (1). For a such given signal $s(t)$, the output of the continuous TKEO, denoted by Ψ, yields the following expression (Maragos P. et al., 1993):

$$\Psi[s(t)] = [\dot{s}(t)]^2 - s(t)\ddot{s}(t) \tag{1}$$

where $\dot{s}(t)$ and $\ddot{s}(t)$ denote the first and the second time derivatives of $s(t)$ respectively. Under realistic conditions (Maragos et al., 1993), when applied to AM-FM signal $s(t) = a(t)\cos(\phi(t))$, the 1D TKEO yields as output $\Psi[s(t)] \approx [a(t)\dot{\phi}(t)]^2$. Thus the local envelope $a(t)$ and the instantaneous frequency $\dot{\phi}(t)$ can be estimated using the energy separation algorithm (ESA) (Maragos et al., 1993):

$$|\dot{\phi}(t)| \approx \sqrt{\frac{\Psi[\dot{s}(t)]}{\Psi[s(t)]}};\ |a(t)| \approx \frac{\Psi[s(t)]}{\sqrt{\Psi[\dot{s}(t)]}} \tag{2}$$

A discrete TKEO, applied to a differentiated signal, called FSA, has been used in WSLI (Larkin, 1996). This operator, as well useful for n-D demodulation, has been extended to multidimensional signals (Maragos and Bovik, 1995; Boudraa et al., 2005; Larkin, 2005), also using directional derivatives (Salzenstein et al., 2013). It can be effective to improve the fineness of the information, by combining other approaches, such as a correlation technique (Salzenstein et al., 2014). In this study, we exploit TKEO, in order to initialize our B-spline estimation algorithm.

4 Summary of the B-spline model

We propose to model the surface parameters by B-splines. This piecewise polynomial approach was introduced in (Schoenberg, 1946). The linear combination of these functions allows to express a continuous function with a countable set of variables, called control points. Defining the set of B-spline basis functions require two elements:

- a degree d (or order $d+1$), that specifies the maximal degree of the polynomial functions;
- a knot vector $\mathbf{k}$ that is a sequence of increasing real numbers, i.e., $k = \{k_0, k_1, k_K\}$, with $k_0 \leq k_1 ... \leq k_K$.

Considering $K+1$ nodes, a polynomial function of degree d is defined between two consecutive nodes. A B-spline basis function of degree d comprises $d+2$ consecutive nodes from the vector $\mathbf{k}$. The number of B-spline basis functions of degree d is thus equal to $M = K - d$. Let $b_m^d(x)$, where $m \in \{1, ..., M\}$, be the mth B-spline basis function of degree d defined on $k_m, ..., k_{m+d+1}$ for a given variable x. The Cox de Boor algorithm (De Boor, 1972), generates B-spline basis by recurrence formula:

$$b_m^0(x) = \begin{cases} 1 & \text{if} \quad k_m \leq x < k_{m+1} \\ 0 & \text{otherwise} \end{cases}$$

$$b_m^d(x) = \frac{x - k_m}{k_{m+d} - k_m} b_m^{d-1}(x) + \frac{k_{m+d+1} - x}{k_{m+d+1} - k_{m+1}} b_{m+1}^{d-1}(x)$$

An alternative method consist in applying d convolution, such that:

$$b_m^d(x) = \underbrace{b_m^0 * b_m^0 * ... * b_m^0}_{d \text{ times}}(x)$$

Among the remarkable properties of B-splines, let us highlight i) locality of their support i.e, $b_m^d(x) = 0\ \forall\ x \notin [k_m, k_{m+d+1}]$; ii) nullity of the values at extremities of their interval i.e, $b_m^d(k_m) = b_m^d(k_{m+d+1}) = 0$; iii) non negativity i.e, $\forall x\ b_m^d(x) \geq 0$; iv) normalized sum for non-zero functions on a knot interval i.e., $\sum_{m=1}^{M} b_m^d(x) = 1\ \forall\ x \in [k_m, k_{m+1}]$; v) B-spline functions are related to $\mathcal{C}^d$ class of continuity, on a knot interval $[k_m, k_{m+d+1}]$. A uniform knot vector, formed by equally spaced knots, helps to provide B-spline basis functions as shifted versions of each others: $\forall\ m\ \in \{1, 2, ..., M\}, b_m^d(x) = b_0^d(x - k_m)$. It is possible to construct B-spline functions $M = K - d$ of degree d, defined on a vector of knots containing $K+1$ elements, taking into account the knots coinciding at the extremities.

5 Characteristics of interferometric data modeled by B-splines

An interpolation or approximation problem yields to a B-spline curve $f(x)$ expressed in the following way:

$$f(x) = \sum_{m=1}^{M} u_m b_m^d(x), \tag{3}$$

where $u_m \in \mathbb{R}$ is a control point (called also 'weights') of the mth B-spline basis function $b_m^d(x)$. Given $\mathbf{b}[x] = \left[b_1^d(x)\ b_2^d(x)\ ...\ b_M^d(x)\right]^T$ and $\mathbf{u} = [u_1 ... u_M]$ Eq. (3) yields to a vector characterization:

$$f(x) = \mathbf{b}[x]^T \mathbf{u} \tag{4}$$

We process the volume of data, described in section 2 by proceeding slice by slice, corresponding to 2D signals $s(z, i)$, denoted by $s_i(z)$, say of size $N \times I$ where N is the length of the optical axis (commonly called z-axis) and I is the maximum size of the lateral axis

i (commonly called x-axis). For a given set of J surfaces or layers of material, an interferometric model may be expressed in a following way by considering an additive noise $n_i(z)$

$$\begin{aligned} s_i(z) &= \sum_{j=1}^{J} a_{ij} \exp\left[-\frac{(z-c_{ij})^2}{2\sigma_{ij}^2}\right] \\ &\quad \times \cos\left(2\pi\nu_{ij}\left(z-c_{ij}\right)\right) + n_i(z) \end{aligned}$$

which could be condensed using a parametric function ϕ, including Gaussian and carrier, as follows:

$$s_i(z) = \sum_{j=1}^{J} a_{ij}\phi(z-c_{ij};\sigma_{ij};\nu_{ij}) + n_i(z) \quad (5)$$

Hence, each surface of the material, labeled by j could be estimated by a set of centers $\left\{c_{1j}, c_{2j}, ..., c_{Ij}\right\}$. In other words, for each lateral position i the peak related to a class j is parameterized along the optical axis z, by its center c_{ij}, amplitude a_{ij} and standard deviation σ_{ij}, at a given carrier frequency ν_{ij}. This is summed up in a vectorized form:

$$\mathbf{s}_i = \sum_{j=1}^{J} a_{ij}\Phi(c_{ij};\sigma_{ij};\nu_{ij}) + \mathbf{n}_i \quad (6)$$

In our model, extended (Mortada et al., 2018), under an assumption of locally smooth surfaces, we assume that all characteristic parameters c_{ij}, a_{ij}, σ_{ij}, ν_{ij} parameters are modeled by B-splines defined on the same knot vector k, with unknown control points. Considering knot positions on discrete values, yields:

$$\forall\ j,\ a_{ij} = a_j(i) = \sum_{m=1}^{M} A_m^j b_m^d(i) = \mathbf{b}[i]^T \mathbf{A}_j \quad (7)$$

$$\forall\ j,\ c_{ij} = c_j(i) = \sum_{m=1}^{M} C_m^j b_m^d(i) = \mathbf{b}[i]^T \mathbf{C}_j \quad (8)$$

$$\forall\ j,\ \sigma_{ij} = \sigma_j(i) = \sum_{m=1}^{M} \Sigma_m^j b_m^d(i) = \mathbf{b}[i]^T \mathbf{\Sigma}_j \quad (9)$$

$$\forall\ j,\ \nu_{ij} = \nu_j(i) = \sum_{m=1}^{M} V_m^j b_m^d(i) = \mathbf{b}[i]^T \mathbf{V}_j \quad (10)$$

where $\mathbf{A} = \left[A_1^j, A_2^j, ..., A_M^j\right]^T$, $\mathbf{C}$, $\mathbf{\Sigma}$, $\mathbf{V}$ respectively define the control points related to the amplitude, surface position, gaussian shape and carrier frequency, whereas $\mathbf{b}[i]^T = \left[b_1^d(i)\ b_2^d(i)\ ...\ \right]$ being a vector gathering the B-splines evaluated at the mixture index i. Finally, the proposed model approximating the interferometric signal $\mathbf{s}_i$ by means of B-splines becomes:

$$\forall i, \mathbf{s}_i = \sum_{j=1}^{J} \mathbf{b}[i]^T \mathbf{A}_j \Phi\left[\mathbf{b}[i]^T; \mathbf{C}_j; \mathbf{\Sigma}_j; \mathbf{V}_j\right] + \mathbf{n}_i \quad (11)$$

Under Gaussian noisy assumption, the maximum likelihood estimation of the control points parameters, leads to the minimization of the following function:

$$\mathcal{L}(\Theta) = \sum_i \left\| \mathbf{s}_i - \sum_{j=1}^{J} \mathbf{b}[i]^T \mathbf{A}_j \Phi\left[\mathbf{b}[i]^T; \mathbf{C}_j; \mathbf{\Sigma}_j; \mathbf{V}_j\right] \right\|^2$$

where $\Theta = (\mathbf{A}, \mathbf{C}, \mathbf{\Sigma}, \mathbf{V})$. In order to solve the nonlinear least square minimization problem $\min_\Theta \mathcal{L}(\Theta)$, as in (Mortada et al., 2018), a Sequential Quadratic Programming (SQP) algorithm (Nocedal and Wright, 1999) could be helpful. However, to enhance robustness in certain situations we have tested (synthetic and real data), a classic simulated annealing algorithm, moving the control points, proves its effectiveness. We have implemented it, in combination with the Teager-Kaiser to enhance parameter initialization.

6 Results

6.1 Synthetic data and images

We illustrate the proposed model and its robustness on synthetic data, synthetic and real interferometric images. Fig. 3-4 show initial and estimated data related to the four parameters of interest, for a signal-to-noise ratio of 20 dB, respectively in the context of one class and two classes, by the method SQP. The number of control points respectively equals $7, 6, 7, 6$ concerning the surfaces, amplitudes, variances, and frequencies. These examples make relevant the possibility of exploiting B-splines by means of our interferometric model. Fig. 5,6,7,8,9,10 deal with synthetic interferometric images and their estimates, for which the initial data were simulated by smoothing randomly initial data (produced by stochastic process). In a context of relatively low SNR (5 dB), the quantitative performances of the Teager-Kaiser method and B-Splines are reported in tables 1 and 2. We have processed Teager-Kaiser technique to initialize our method, followed by a simulated annealing approach. The combination of both techniques allows a better convergence of the algorithm, while improving the estimation for all characteristic parameters. The number of control points is respectively 41 for estimating the surfaces, and 21 for the other parameters. In particular, the algorithm based on B-splines significantly reduces the error rate of variances and frequencies, which shows, in this context, that regularization taking into account neighboring information over all the parameters, contributes to a better estimation of the surface.

6.2 Real interferometric images

Finally, as illustrated in Fig.11, Fig.12 we have applied the previous algorithm to real interferometric images. Fig.11 shows a silicon surface that both algorithms process in a relatively similar manner, the B-spline method estimating the frequencies better (in the real image, these are much more continuous than the TK algorithm suggests) and, as expected, slightly smoothing the data produced by TKEO. Each parameter is estimated using $P = 36$ control points. Let us note the relatively high noise level by observing the profile Fig.11(b). Fig.12 shows the effectiveness of the method applied to the detection of a oil drop, for which certain areas of the image, very noisy, make the Teager-Kaiser algorithm almost inoperative. The resulting surface of the B-spline approach corrects this drawback, and perfectly matches the shape of the oil-drop. Under a relevant assumption, the carrier frequency fluctuating quite little, the order of the B-spline regarding frequencies was set to 3 (second order polynomial). This allows us to obtain a more stable estimate than the TKEO. On the other hand, both approaches determine a decreasing amplitude (the appearance of the oil-drop interference signal being empirically attenuated in the right part of the image), which makes it compatible, at constant frequency, with an increasing variance (spreading out Gaussian envelope). Finally, the relative small number of control points (8 for surface, amplitude and variance, 6 for frequency) seems appropriate for this very smooth surface. Finally, let us note that the average calculation time for an 256x256 image corresponds to 15 seconds (Matlab2022, cpu Intel Core i5-7300U 2.6 GHz, Ram 16Go).

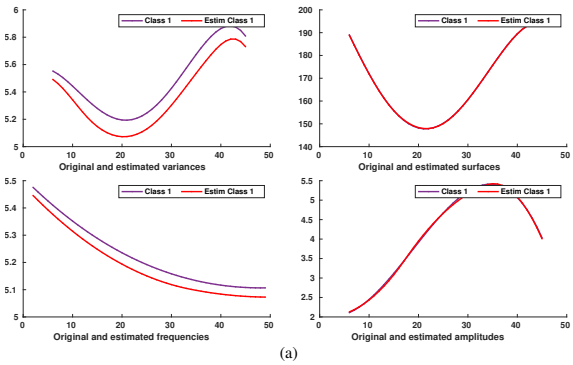

(a)

Figure 3: (a): One class data (in blue) and their estimation (in red) by cubic B-spline (variance, surface, frequency, amplitude) with knot vector $k = [1,1,1,1,1.7,20.5,30.2,50,50,50,50]$; the number of control points being respectively $7,6,7,6$.

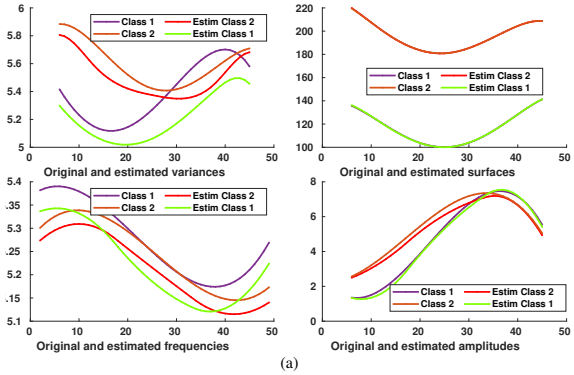

(a)

Figure 4: (a): Two classes data (resp. in purple and brown) and their estimation (resp. in green and red) by cubic B-spline (variance, surface, frequency, amplitude) with knot vector $k = [1,1,1,1,10.7,20.5,30.2,50,50,50,50]$; the number of control points being respectively $7,6,7,6$.

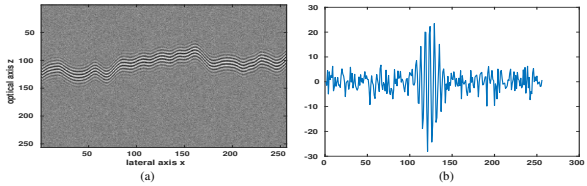

(a) (b)

Figure 5: (a): Synthetic interferometric signal; (b) profile signal along the optical axis;

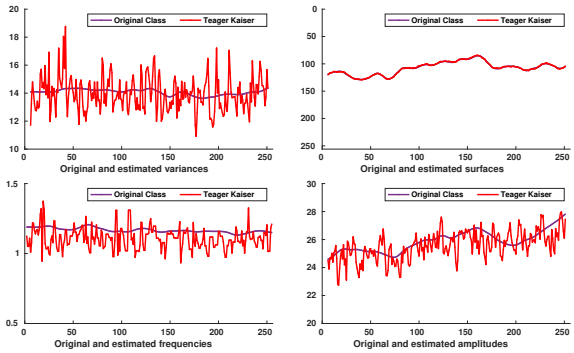

Figure 6: original (in blue) and estimated parameters (in red) of Fig. 5(a) with Teager-Kaiser (from top left to bottom right: variance, surface, frequency, amplitude).

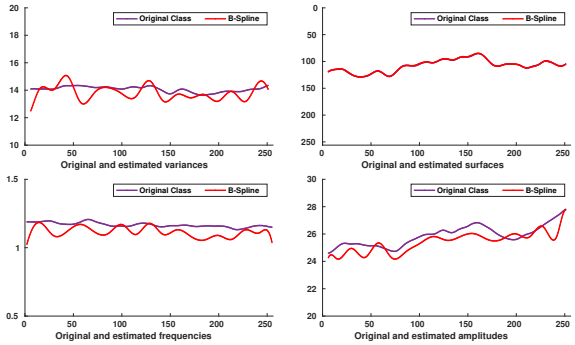

Figure 7: original (in blue) and estimated parameters (in red) of Fig. 5(a) with B-Spline technique (from top left to bottom right: variance, surface, frequency, amplitude).

Table 1: Fig. 6, 7 : error rates estimation (%) for each characteristic, for TK alone and then combined with B-Spline.

	surface	amplitude	variance	frequency
Teager-Kaiser	0.37	2.63	6.77	6.78
TK + B-Spline	0.27	1.98	2.82	4.37

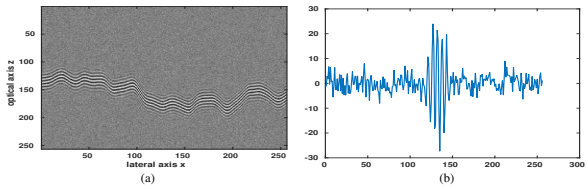

Figure 8: (a): Synthetic interferometric signal; (b) profile signal along the optical axis; .

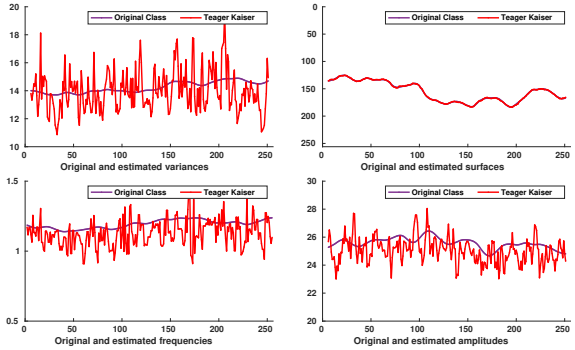

Figure 9: original (in blue) and estimated parameters (in red) of Fig. 8(a) with Teager-Kaiser (from top left to bottom right: variance, surface, frequency, amplitude).

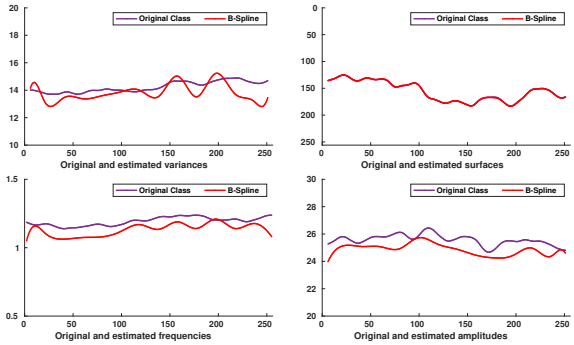

Figure 10: original (in blue) and estimated parameters (in red) of Fig. 8(a) with B-Spline technique (from top left to bottom right: variance, surface, frequency, amplitude).

Table 2: Fig. 9, 10 : error rates estimation (%) for each characteristic, for TK alone and then combined with B-Spline.

	surface	amplitude	variance	frequency
Teager-Kaiser	0.53	3.31	8.27	7.68
TK + B-Spline	0.33	2.76	3.77	4.92

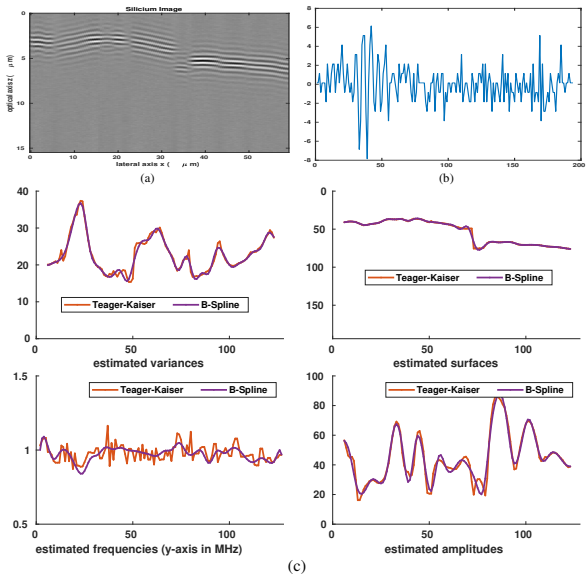

Figure 11: (a): Real interferometric image and its profile (b) along the optical axis; (c): estimated parameters with B-Splines (in blue) and Teager-Kaiser (in red): from top left to bottom right: variance, surface, frequency, amplitude.

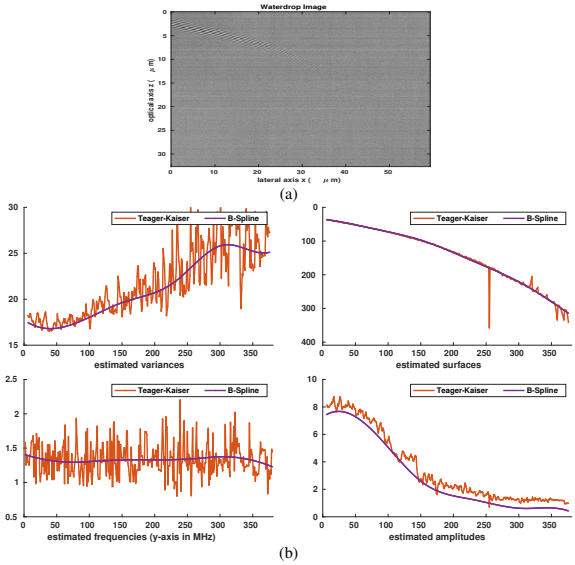

Figure 12: (a): oil-drop interferometric image; (b): estimated parameters with B-Splines (in blue) and Teager-Kaiser (in red): from top left to bottom right: variance, surface, frequency, amplitude.

7 Conclusion

In this paper, we have introduced a new method for tracking material surfaces, combining two types of approaches: a nonlinear Teager-Kaiser operator, and a model based on B-splines, allowing a regularization taking into account the neighboring points of the surface according to four parameters capable of characterizing a fringe signal. After initialization using TKEO, we estimate the control points by a simulated annealing procedure. Although our assumption is suitable for relatively smooth surfaces, we have provided promising quantitative and also qualitative results. We have illustrated the performance of our method on synthetic and real images, showing its ability to match the roughness of the surfaces. A possible extension of our algorithm could concern, on the one hand, an initialization step (by TKEO or another operator) more adapted to noisy data. On the other hand, the consideration of other image slices within the 3D data cube (neighboring xz sections) to help initialization, and also enrichment of the model by using more complex splines choosing locally different orders for each parameter or, for example, using P-spline model. The relatively fast processing, which can be parallelized (more efficient simulated annealing etc), an interactive procedure would make it possible to optimize the suitable number of splines. For an automatic procedure, this number depending on each parameter, could be based on machine learning adapted to data similar to those being processed.

8 Acknowledgment

We would like to thank Mr. Freddy Anstotz and Mr. Christophe Cordier from the IPP laboratory, for providing the interferometric images.

REFERENCES

Boudraa, A.-O. and Salzenstein, F. (2018). Teager–kaiser energy methods for signal and image analysis: A review. *Digital Signal Processing*, 78:338–375.

Boudraa, A.-O., Salzenstein, F., and Cexus, J.-C. (2005). Two-dimensional continuous higher-order energy operators. *Optical Engineering*, 44(11):117001–117001.

Bruno, L. (2007). Global approach for fitting 2d interferometric data. *Optics Express*, 15(8):4835–4847.

Chim, S. S. and Kino, G. S. (1990). Correlation microscope. *Optics Letters*, 15(10):579–581.

De Boor, C. (1972). On calculating with b-splines. *Journal of Approximation theory*, 6(1):50–62.

de Groot, P., de Lega, X. C., Kramer, J., and Turzhitsky, M. (2002). Determination of fringe order in white-light interference microscopy. *Applied optics*, 41(22):4571–4578.

de Groot, P. and Deck, L. (1993). Three-dimensional imaging by sub-nyquist sampling of white-light interferograms. *Optics Letters*, 18(17):1462–1464.

Duan, Y., Li, Z., and Zhang, X. (2023). Least-squares phase-shifting algorithm of coherence scanning interferometry with windowed b-spline fitting, resampled and subdivided phase points for 3d topography metrology. *Measurement*, 217:113103.

Gianto, G., Salzenstein, F., and Montgomery, P. (2016). Comparison of envelope detection techniques in coherence scanning interferometry. *Applied Optics*, 55(24):6763–6774.

Guo, T., Ma, L., Chen, J., Fu, X., and Hu, X. (2011). Microelectromechanical systems surface characterization based on white light phase shifting interferometry. *Optical Engineering*, 50(5):053606–053606.

Gurov, I., Ermolaeva, E., and Zakharov, A. (2004). Analysis of low-coherence interference fringes by the kalman filtering method. *Journal of the Optical Society of America A*, 21(2):242–251.

Gurov, I. and Volynsky, M. (2012). Interference fringe analysis based on recurrence computational algorithms. *Optics and Lasers in Engineering*, 50(4):514–521.

Hoch, M., Fleischmann, G., and Girod, B. (1994). Modeling and animation of facial expressions based on b-splines. *The Visual Computer*, 11:87–95.

Larkin, K. G. (1996). Efficient nonlinear algorithm for envelope detection in white light interferometry. *Journal of the Optical Society of America A*, 13(4):832–843.

Larkin, K. G. (2005). Uniform estimation of orientation using local and nonlocal 2-d energy operators. *Optics Express*, 13(20):8097–8121.

Mallat, S. and Zhong, S. (1992). Characterization of signals from multiscale edges. *IEEE Transactions on Pattern Analysis & Machine Intelligence*, 14(07):710–732.

Maragos, P. and Bovik, A. C. (1995). Image demodulation using multidimensional energy separation. *Journal of the Optical Society of America A*, 12(9):1867–1876.

Maragos, P., Kaiser, J. F., and Quatieri, T. F. (1993). Energy separation in signal modulations with application to speech analysis. *IEEE Transactions on Signal Processing*, 41(10):3024–3051.

Maragos P., Kaiser J.F., and QuatieriT.F. (1993). On amplitude and frequency demodulation using energy operators. *IEEE Transactions on Signal Processing*, 41(4):1532–1550.

Medioni, G. and Yasumoto, Y. (1987). Corner detection and curve representation using cubic b-splines. *Computer vision, graphics, and image processing*, 39(3):267–278.

Montgomery, P. C., Salzenstein, F., Montaner, D., Serio, B., and Pfeiffer, P. (2013). Implementation of a fringe visibility based algorithm in coherence scanning interferometry for surface roughness measurement. In *Optical Measurement Systems for Industrial Inspection VIII*, volume 8788, pages 951–961. SPIE.

Mortada, H., Mazet, V., Soussen, C., and Collet, C. (2018). Spectroscopic decomposition of astronomical multispectral images using b-splines. In *2018 9th Workshop on Hyperspectral Image and Signal Processing: Evolution in Remote Sensing (WHISPERS)*, pages 1–5. IEEE.

Nocedal, J. and Wright, S. J. (1999). *Numerical optimization*. Springer.

O'Mahony, C., Hill, M., Brunet, M., Duane, R., and Mathewson, A. (2003). Characterization of micromechanical structures using white-light interferometry. *Measurement Science and Technology*, 14(10):1807.

Pavliček, P. and Michalek, V. (2012). White-light interferometryenvelope detection by hilbert transform and influence of noise. *Optics and Lasers in Engineering*, 50(8):1063–1068.

Reinsch, C. H. (1967). Smoothing by spline functions. *Numerische mathematik*, 10(3):177–183.

Rueckert, D., Aljabar, P., Heckemann, R. A., Hajnal, J. V., and Hammers, A. (2006). Diffeomorphic registration using b-splines. In *Medical Image Computing and Computer-Assisted Intervention–MICCAI 2006: 9th International Conference, Copenhagen, Denmark, October 1-6, 2006. Proceedings, Part II 9*, pages 702–709. Springer.

Salzenstein, F. and Boudraa, A.-O. (2009). Multidimensional higher order differential operators derived from the Teager-Kaiser energy tracking function. *Signal Processing*, 89(4):623–640.

Salzenstein, F., Boudraa, A.-O., and Chonavel, T. (2013). A new class of multi-dimensional teager-kaiser and higher order operators based on directional derivatives. *Multidimensional Systems and Signal Processing*, 24:543–572.

Salzenstein, F., Montgomery, P., and Boudraa, A.-O. (2014). Local frequency and envelope estimation by teager-kaiser energy operators in white-light scanning interferometry. *Optics Express*, 22(15):18325–18334.

Sandoz, P. (1997). Wavelet transform as a processing tool in white-light interferometry. *Optics Letters*, 22(14):1065–1067.

Schoenberg, I. J. (1946). Contributions to the problem of approximation of equidistant data by analytic functions. part b. on the problem of osculatory interpolation. a second class of analytic approximation formulae. *Quarterly of Applied Mathematics*, 4(2):112–141.

Unser, M. (1999). Splines: A perfect fit for signal and image processing. *IEEE Signal processing magazine*, 16(6):22–38.

Vakman D. (1996). On the analytic signal, the Teager-Kaiser energy algorithm, and other methods for defining amplitude and frequency. *IEEE Transactions on Signal Processing*, 44(4):791–797.

Wielgus, M., Patorski, K., Etchepareborda, P., and Federico, A. (2014). Continuous phase estimation from noisy fringe patterns based on the implicit smoothing splines. *Optics Express*, 22(9):10775–10791.

Zhu, P. and Wang, K. (2012). Single-shot two-dimensional surface measurement based on spectrally resolved white-light interferometry. *Applied optics*, 51(21):4971–4975.